DOI: 10.12923/cipms-2026-0018 Curr. Issues Pharm. Med. Sci., Vol. 39, No. 2, Pages 109-117

Current Issues in Pharmacy and Medical Sciences
Formerly ANNALES UNIVERSITATIS MARIAE CURIE-SKLODOWSKA, SECTIO DDD, PHARMACIA

journal homepage: https://czasopisma.umlub.pl/curipms



Combined effects of photobiomodulation and Ag/$LaVO_4$:Eu^{3+} nanocomposite hydrogel on wound re-epithelialization: association with endothelial activation and keratinocyte-related amphiregulin signaling

Sergey Pavlov[1], Marina Kumetchko[1*], Olga Litvinova[1], Nataliia Babenko[1], Vladimir Klochkov[2], Svitlana Yefimova[2], Igor Kolisnyk[3]

[1] Department of Surgery No. 4, Kharkiv National Medical University, Kharkiv, Ukraine
[2] Yu.V. Malyukin Department of Nanostructured Materials, Institute for Scintillation Materials, NAS of Ukraine, Kharkiv, Ukraine
[3] Department of Human Anatomy, Clinical Anatomy and Operative Surgery, Kharkiv National Medical University, Kharkiv, Ukraine

ARTICLE INFO

Received 19 March 2026
Accepted 10 June 2026

Keywords:
keratinocyte proliferation;
nanoparticles;
photobiomodulation;
tissue regeneration;
wound healing.

ABSTRACT

In this study, a combined therapeutic strategy integrating photobiomodulation (PBM) with an antibacterial hydrogel containing silver nanoparticles and europium-activated lanthanum orthovanadate nanoparticles (Ag/$LaVO_4^{3+}$ NPs) was developed to enhance wound healing. This integrated approach was designed to provide complementary effects by simultaneously improving antibacterial activity and promoting tissue regeneration. The study aimed to investigate the roles of vascular cell adhesion molecule-1 (VCAM-1), endothelin-1 (ET-1), and keratinocyte autocrine factor (KAF) in reparative processes occurring in chronic wounds following treatment with Ag/$LaVO_4^{3+}$ NPs hydrogel and PBM therapy. Thirty WAG rats were randomly assigned to five groups: Con, Gel (Ag/$LaVO_4^{3+}$ NPs hydrogel), PBM (660 nm, 50 mW, 1 J/cm^2), Gel+PBM, and intact. Chronic wounds were induced, and serum levels of VCAM-1, ET-1, and KAF were determined using enzyme-linked immunosorbent assay (ELISA). In addition, histological analysis was performed. Experimental wounds were associated with elevated serum levels of VCAM-1 and ET-1 in the control animals, which is consistent with endothelial activation under inflammatory conditions. PBM therapy reduced the levels of these markers, whereas the combined Gel+PBM treatment produced the most pronounced effect, suggesting a greater attenuation of endothelial activation and the establishment of conditions favorable for wound healing. Serum KAF levels exhibited only a transient increase on day 3 in the control group and remained unchanged in the treated groups. The combination of PBM therapy and Ag/$LaVO_4^{3+}$ NPs hydrogel was associated with reduced ET-1 and VCAM-1 levels, consistent with attenuated endothelial activation during wound healing. These changes were accompanied by improved re-epithelialization; however, the underlying mechanisms require further investigation.

INTRODUCTION

Currently, the problem of chronic wound healing remains unresolved. Approximately 4% of the world's population suffers from skin ulcers [1]. According to other reports, 1-2% of individuals in developed countries are affected by chronic wounds [2]. This prevalence is associated with population aging, concomitant diseases, hormonal and nutritional disorders, and other contributing factors [3]. The global economic burden of wound care reached $148.65 billion in 2022 [4]. In addition, chronic wounds substantially impair patients' quality of life.

Wound healing is a complex cellular process that occurs through sequential and overlapping phases, including inflammation, proliferation, and remodeling, and involves intricate interactions among growth factors and cytokines. Disruption of these interactions may lead to the development of chronic wounds. Moreover, factors such as population aging, chronic diseases, increasing antimicrobial resistance,

* **Corresponding author**
e-mail: cndl@med.edu.ua

© 2026 Author(s). This is an open access article distributed under the Creative Commons Attribution-NonComercial-No Derivs licence (http://creativecommons.org/licenses/by-nc-nd/4.0/)

and injuries sustained during military operations adversely affect treatment outcomes. These challenges necessitate the development of novel and effective approaches to optimize the repair process. Among the promising strategies for wound management are photobiomodulation (PBM) therapy and nanomaterials.

PBM therapy is considered an effective and safe approach for the treatment of wounds and scars, as well as neurological and psychological disorders, dental conditions, and other diseases [5]. PBM modulates cellular metabolism through interactions with mitochondrial cytochromes, resulting in increased oxygen consumption, adenosine triphosphate (ATP) production, and reactive oxygen species (ROS) generation, while also regulating nitric oxide (NO) release and intracellular Ca^{2+} concentrations [6]. Consequently, PBM activates secondary signaling pathways involved in angiogenesis, collagen synthesis, and growth factor release, thereby promoting wound healing. However, the therapeutic effects of PBM are highly dependent on the dose-response relationship. Therefore, parameters such as wavelength, energy density, and irradiation time should be carefully optimized.

Hydrogels provide an optimal environment for wound healing. Furthermore, the incorporation of therapeutic nanoparticles and biomolecules into hydrogel matrices can enhance and accelerate tissue repair. For example, silver nanoparticles (Ag NPs) exhibit potent antibacterial, antimicrobial, and anti-inflammatory properties, which play a crucial role in wound healing [7]. Released Ag^+ ions disrupt microbial cell membranes and DNA, thereby preventing infection and biofilm formation [8]. In addition, Ag NPs reduce the levels of pro-inflammatory cytokines, including interleukin-1β (IL-1β), tumor necrosis factor-α (TNF-α), and IL-6, and enhance the production of vascular endothelial growth factor (VEGF) and and transforming growth factor-β (TGF-β), which stimulate angiogenesis and promote the migration of fibroblasts and keratinocytes [9].

Europium-activated lanthanum orthovanadate nanoparticles ($LaVO_4^{3+}$ NPs) possess dual biological activity, acting either as antioxidants or pro-oxidants depending on the environmental conditions [10]. Their antioxidant activity is attributed to the ability of vanadium ions within the crystal lattice to participate in reversible redox reactions, thereby scavenging electrons and neutralizing reactive oxygen species. This effect reduces oxidative stress, attenuates inflammation, and promotes the transition from the inflammatory to the regenerative phase of wound healing [11]. Under conditions of severe oxidative stress or at high concentrations, these nanoparticles may enhance ROS generation, leading to cellular damage and increased apoptosis [12]. In addition, $LaVO_4^{3+}$ NPs exhibit antimicrobial activity, making them promising candidates for antibacterial applications [13].

In the present study, we attempted to achieve optimal therapeutic outcomes by combining PBM therapy with an antibacterial hydrogel containing silver nanoparticles and europium-activated lanthanum orthovanadate nanoparticles (Ag/$LaVO_4^{3+}$ NPs). This combined approach was designed to take advantage of the beneficial properties of both treatment modalities and to enhance their individual effects, thereby improving wound healing and tissue regeneration.

The aim of this study was to investigate the roles of vascular cell adhesion molecule-1 (VCAM-1), endothelin-1 (ET-1), and keratinocyte autocrine factor (KAF) in the reparative processes associated with chronic wound healing following treatment with a hydrogel containing silver nanoparticles and europium-activated lanthanum orthovanadate nanoparticles in combination with PBM therapy.

MATERIALS AND METHODS

Chemicals

Lanthanum chloride ($LaCl_3 \cdot 7H_2O$, 99.9%), sodium metavanadate ($NaVO_3$, 96%), silver nitrate ($AgNO_3$, 99%), sodium tetraborate ($Na_2B_4O_7 \cdot 10H_2O$, 98%), and disodium EDTA (EDTA·2Na, 99.8%) were purchased from Acros Organics (USA). Glycerol (>99.5%) and Carbomer 940 were obtained from Sigma-Aldrich (USA).

Synthesis of $LaVO_4^{3+}$ nanoparticles

$LaVO_4^{3+}$ nanoparticles were prepared as an aqueous colloidal dispersion using a wet-chemical approach [14,15]. During the synthesis, disodium EDTA was used as a stabilizing agent, imparting a negative surface charge to the nanoparticles. Upon completion of the reaction, the colloidal dispersion was purified by dialysis against deionized water for 24 h using a membrane with a molecular weight cut-off of 12 kDa to remove residual ions and organic impurities. The purified colloid exhibited long-term stability and retained its physicochemical properties for more than two years when stored in sealed ampoules at room temperature.

Synthesis of silver nanoparticles

Silver nanoparticles (Ag NPs) were synthesized by mixing 120 mL of a 0.001 M $AgNO_3$ solution with 60 mL of a 0.0015 M EDTA solution in a 200 mL glass beaker, followed by magnetic stirring for 10 min. Subsequently, 8 mL of 0.02 M NaOH was added dropwise under continuous stirring, resulting in an alkaline medium with a pH of approximately 12.0-12.5. The reaction mixture was then transferred to a thermostatically controlled water bath equipped with an overhead stirrer and heated at 90°C for 20 min. The formation of silver nanoparticles was monitored by UV-Vis spectroscopy. A gradual change in the color of the solution to yellowish-brown was observed. After cooling, a characteristic localized surface plasmon resonance band appeared in the 400-430 nm region, confirming the successful formation of Ag NPs [16].

Preparation of the Ag/$LaVO_4^{3+}$ nanoparticle hydrogel

An aqueous dispersion of $LaVO_4^{3+}$ nanoparticles (46 mL, 3.9 g/L) was transferred to a 300 mL beaker, followed by the addition of 2.00 g of Carbomer 940. The mixture was stirred magnetically and allowed to hydrate at room temperature for 24 h. Subsequently, 145 mL of an aqueous Ag NP suspension (0.076 g/L) and 20 mL of distilled water were added, and the resulting mixture was stirred for an additional 15 min.

Gelation was initiated by the gradual addition of 12 mL of a 4% (w/v) sodium tetraborate ($Na_2B_4O_7$) solution prepared in glycerol under vigorous stirring. This procedure resulted in the formation of a homogeneous hydrogel with the

following final composition: $LaVO_4^{3+}$ nanoparticles, 0.8 g/L; Ag NPs, 0.049 g/L; $Na_2B_4O_7$, 2.15 g/L; glycerol, 65.6 g/L; and Carbomer 940, 8.96 g/L.

The resulting hydrogel exhibited good storage stability for at least 12 months when stored at 15-25°C and protected from direct light.

Instrumentation and characterization

The morphology and particle size of the synthesized nanoparticles were examined by transmission electron microscopy (TEM) using a JEOL JEM-2100F microscope equipped with a Schottky field-emission gun and operated at an accelerating voltage of 200 kV. Optical absorption measurements were performed using a Specord 200 UV-Vis spectrophotometer (Analytik Jena, Germany). The electrokinetic properties of the colloidal dispersions were evaluated by zeta potential measurements carried out using a ZetaPALS/BIMAS analyzer (Brookhaven Instruments Corp., USA) operating in phase analysis light scattering mode.

Animals

The study involved 30 WAG rats bred in the vivarium of Kharkiv National Medical University. The animals were 8 months old on average and had a mean body weight of 230 g. They were housed under standard laboratory conditions. The rats were randomly allocated to five groups, each consisting of six animals. The intact group (Int) comprised healthy rats that were not subjected to any intervention. The control group (Con) consisted of animals with wound defects. Experimental group 1 (Gel) included animals with wound defects treated with $Ag/LaVO_4^{3+}$ NPs hydrogel. Experimental group 2 (PBM) consisted of animals with wound defects treated with PBM therapy. Experimental group 3 (Gel+PBM) included animals with wound defects treated with a combination of $Ag/LaVO_4^{3+}$ NPs hydrogel and PBM therapy.

Creation of a wound defect

Wound defects were induced in animals belonging to the control and experimental groups. Before surgery, the rats were anesthetized with zolazepam (tiletamine hydrochloride and zolazepam hydrochloride; Virbac, France) administered at a dose of 10 mg/kg body weight. The dorsal skin was depilated, and a circular full-thickness wound with a diameter of 2 cm was created.

Application of $Ag/LaVO_4^{3+}$ NPs hydrogel

The wound defects in animals belonging to experimental group 1 were treated with $Ag/LaVO_4^{3+}$ NPs hydrogel, which was applied as a thin layer to the wound surface.

PBM therapy

The wound defects in animals belonging to experimental group 2 were treated with PBM therapy. Irradiation was performed once daily for five consecutive days, beginning one day after wound induction. A Lika-Therapist M laser device (Cherkasy, Ukraine) was used. The irradiation parameters were as follows: wavelength, 660 nm; output power, 50 mW; and energy density, 1 J/cm².

Combined treatment with $Ag/LaVO_4^{3+}$ NPs hydrogel and PBM therapy

The wound defects in animals belonging to experimental group 3 were first treated with $Ag/LaVO_4^{3+}$ NPs hydrogel. Twenty minutes later, PBM therapy was applied using the protocol described above.

Euthanasia and sample collection

Animals were euthanized on days 3, 7, and 14 after wound induction. Blood samples were collected by cardiac puncture, centrifuged, and serum samples were obtained and subsequently stored in a frozen state.

Wound tissue specimens, including the wound margins, were collected for histopathological analysis. The samples were processed using standard histological procedures and stained with hematoxylin and eosin. Microscopic examination was performed using a PrimoStar light microscope (Zeiss, Germany) equipped with a digital camera.

Determination of bioactive molecule concentrations

Serum concentrations of vascular cell adhesion molecule-1 (VCAM-1), endothelin-1 (ET-1), and keratinocyte autocrine factor (KAF) were determined using commercially available ELISA kits (Elabscience, USA) according to the manufacturer's instructions.

Statistical analysis

For each variable, the normality of data distribution was assessed using the Shapiro-Wilk test, visual inspection of histograms, and Q-Q plots. Homogeneity of variances was evaluated using Levene's test. Under the assumptions of normality and homogeneity of variances, the effects of PBM therapy, hydrogel treatment, and their combination on the studied parameters were analyzed using one-way analysis of variance (ANOVA). When statistically significant differences were detected, post hoc comparisons were performed using Tukey's test. In cases where these assumptions were violated, the nonparametric Kruskal-Wallis test was applied, followed by Dunn's post hoc test. For ease of comparison, the data are expressed as mean ± standard error of the mean (SE). Statistical analyses were performed using Statistica 12 software (StatSoft, USA). A p-value of <0.05 was considered statistically significant.

RESULTS

Characteristics of synthesized nanoparticles

The TEM image of synthesized LaVO4:Eu3+ NPs is presented in Figure 1a and reveals rod-like nanoparticles of about 6 × 30 nm size. LaVO4:Eu3+ NPs were found to have a negative surface charge; the ζ-potential was -30.0 ± 2.9 mV. Absorption spectrum of LaVO4:Eu3+ NPs (Figure 2) consists of wide bands in the 260-320 nm spectral range with the maximum centered at 280 nm that corresponds to charge transfer from oxygen ligands to the vanadium atom in the group [17]. The TEM image of Ag NPs is shown in Figure 1b. Ag nanoparticles are spherical in shape with an average size of 16 ± 1.9 nm and have a negative surface charge; the ζ-potential was -15.0 ± 1.7 mV. The absorption spectrum of Ag NPs (Figure 2) consists of wide bands with a maximum

absorption in the 400-430 nm range, which indicates the localization of surface plasmon resonance on Ag NPs [16].

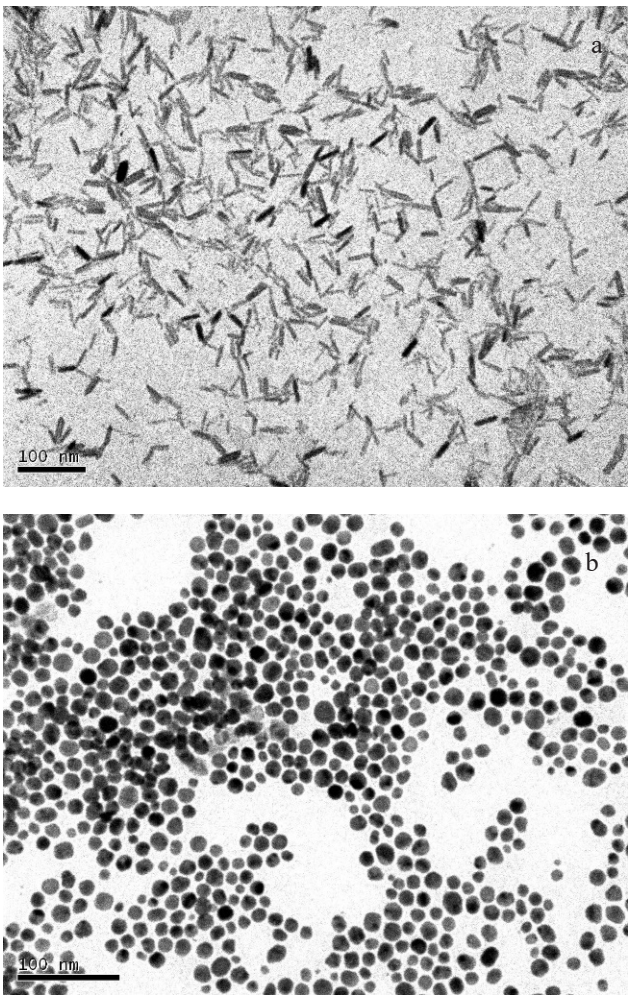

Figure 1. TEM images of synthesized $LaVO_4$:Eu^{3+} NPs (a) and Ag NPs (b)

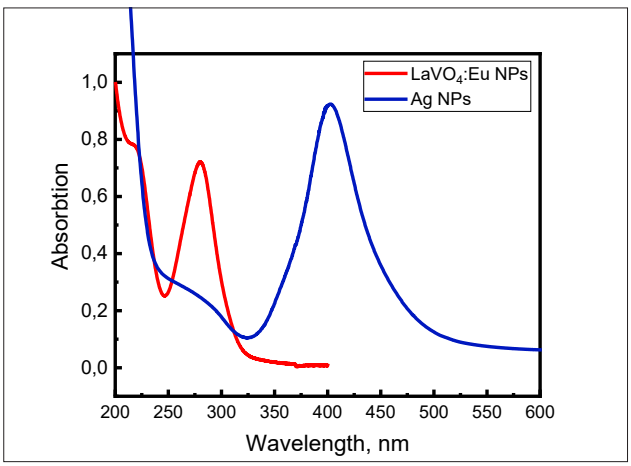

Figure 2. Absorption spectra of $LaVO_4$:Eu^{3+} (red curve) and Ag (blue curve) NPs

Assessment of biomarker levels

Tables 1-3 show the concentrations of the studied indicators in the animals' blood serum on days 3, 7, and 14 of the experiment.

Table 1. Changes in serum VCAM-1 levels in experimental animals

Group	VCAM-1, pg/ml		
	3 days	7 days	14 days
Int	90.284 ± 12.746	90.284 ± 12.746	90.284 ± 12.746
Con	189.139 ± 9.429*	183.301 ± 10.636*	144.126 ± 7.926*
Gel	163.258 ± 8.561*	149.179 ± 8.407*	123.756 ± 8.449
PBM	158.213 ± 8.178*	129.525 ± 8.313*,#	116.185 ± 6.216
Gel+PBM	138.925 ± 8.053*,#	115.482 ± 5.310#	98.885 ± 7.538#

* - differences are significant relative to intact animals; # - the control group, ($p < 0.05$); (n = 6)

Table 2. Changes in serum ET-1 levels in experimental animal

Group	ET-1, pg/ml		
	3 days	7 days	14 days
Int	3.211 ± 0.444	3.211 ± 0.444	3.211 ± 0.444
Con	7.211 ± 0.343*	6.829 ± 0.525*	5.310 ± 0.252*
Gel	6.365 ± 0.437*	5.410 ± 0.411	5.115 ± 0.251*
PBM	5.563 ± 0.225*,#	5.019 ± 0.388	4.296 ± 0.272
Gel+PBM	5.203 ± 0.373*,#	4.610 ± 0.403#	3.703 ± 0.282#

* - differences are significant relative to intact animals; # - the control group, ($p < 0.05$); (n = 6)

Table 3. Changes in serum KAF levels in experimental animals

Group	KAF, pg/ml		
	3 days	7 days	14 days
Int	172.541 ± 7.740	172.541 ± 7.740	172.541 ± 7.740
Con	223.609 ± 11.562*	199.231 ± 5.951	162.836 ± 10.531
Gel	235.241 ± 10.906*	201.082 ± 11.454	195.953 ± 11.756
PBM	217.480 ± 11.971*	211.126 ± 11.734	211.937 ± 21.058
Gel+PBM	252.647 ± 9.980*	225.183 ± 13.159*	162.096 ± 7.362

* - differences are significant relative to intact animals; # - the control group, ($p < 0.05$); (n = 6)

In our study, serum KAF levels in the Con group were increased by 1.30-fold on day 3 compared with those in intact animals ($p < 0.05$). However, no significant differences in KAF concentrations were observed between wounded and intact animals on days 7 and 14 after surgery. Likewise, no significant changes in KAF levels were found in the Gel and PBM groups compared with the Con group ($p > 0.05$) at any stage of the experiment. The greatest increase in KAF concentration relative to the Con group was observed in the Gel+PBM group on days 3 and 7; however, these differences were also not statistically significant ($p > 0.05$).

Serum VCAM-1 levels were elevated in the Con group compared with those in intact animals at all experimental time points ($p < 0.01$). In the Gel group, VCAM-1 concentrations were lower than those observed in the Con group throughout the experiment; however, the differences did not reach statistical significance ($p > 0.05$). PBM therapy resulted in a significant reduction in serum VCAM-1 levels in the PBM group compared with the Con group on day 7 ($p < 0.01$). In addition, lower VCAM-1 concentrations were observed in the PBM group on days 3 and 14, although these differences were not statistically significant ($p > 0.05$). In the Gel+PBM group, serum VCAM-1 levels were significantly lower than those in the Con group at all stages of the experiment ($p < 0.05$).

Serum ET-1 levels were elevated in the Con group compared with those in intact animals throughout the experimental period ($p < 0.001$). In the Gel group, ET-1 concentrations tended to decrease relative to those in the Con group; however, the differences were not statistically significant ($p > 0.05$). In the PBM group, a significant reduction in ET-1 concentration was observed on day 3 compared with the Con group ($p < 0.05$), whereas the decreases observed on days 7 and 14 did not reach statistical significance ($p > 0.05$). Combined treatment with Ag/$LaVO_4^{3+}$ NPs hydrogel and PBM therapy resulted in significantly lower ET-1 levels in the Gel+PBM group compared with the Con group at all stages of the experiment ($p < 0.05$).

Histological analysis of wound tissue

Microscopic examination of the wounds on day 3 revealed signs of the early re-epithelialization process in all groups, manifested by thickening of the basal layer of the epidermis at the wound margins and the initiation of epithelial growth beneath the scab. In the Con group, the wound cavities were filled with fibrin and inflammatory infiltrate composed predominantly of neutrophilic granulocytes and a small number of macrophages. Isolated areas showing signs of fibroblast proliferation and newly formed blood vessels were observed near the wound base (Figure 3a).

In animals from the Gel group, the areas of newly formed granulation tissue were more extensive, occupying up to half of the wound cavity volume. Clusters of fibrin fibers, neutrophils, macrophages, and isolated fibroblasts were observed above these regions (Figure 3b).

In the PBM group, the wound cavities were predominantly filled with immature granulation tissue containing numerous fibroblasts and newly formed capillaries. Some vessels were dilated and engorged with blood, and both perivascular and more extensive hemorrhages were observed (Figure 3c).

Similarly, wounds in animals treated with the combined Gel+PBM regimen were covered with newly formed granulation tissue. A more uniform distribution of fibroblasts and newly formed vessels was observed, and no hemorrhagic areas were detected (Figure 3d).

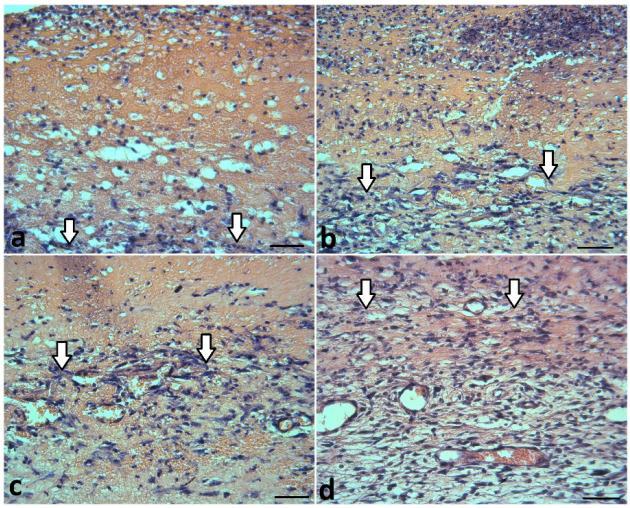

Figure 3. Wound areas in rats on day 3 of the experiment; groups: a) Con, b) Gel, c) PBM, d) Gel+PBM. Areas of granulation tissue growth (arrow). Hematoxylin and eosin. Scale bar 50 μm.

After 7 days, the wound defects in rats from all groups were partially covered with newly formed epidermis and filled with immature granulation tissue. In the Con group, the wounds exhibited signs of pronounced inflammation. The collagen fiber bundles were thin and irregularly arranged, and the distribution of newly formed blood vessels of varying diameters was uneven (Figure 4a). In animals from the Gel group, the cellular component of the granulation tissue consisted predominantly of fibroblasts, accompanied by a small number of neutrophilic granulocytes and macrophages. A uniform distribution of capillaries was observed throughout the granulation tissue (Figure 4b). In the PBM and Gel+PBM groups, the granulation tissue was characterized by a large number of fibroblasts, a low number of leukocytes, and more densely packed collagen fiber bundles arranged predominantly parallel to the wound surface (Figures 4c, 4d). As observed at the previous time point, some blood vessels in the PBM group remained dilated and engorged with blood.

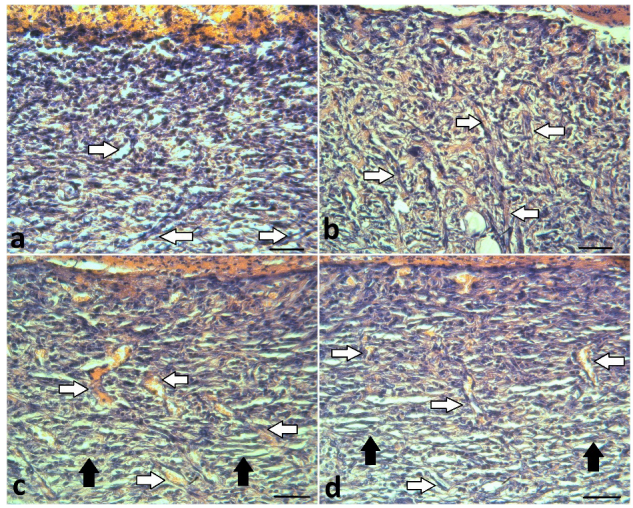

Figure 4. Wound areas in rats on day 7 of the experiment; groups: a) Con, b) Gel, c) PBM, d) Gel+PBM. Capillaries of granulation tissue (white arrow), bundles of densely packed collagen fibers (black arrow). Hematoxylin and eosin. Scale bar 50 μm.

After 14 days, the wound defects in all animals were largely epithelialized and filled with maturing granulation tissue. Moderate leukocyte infiltration persisted in the Con group. In the Gel group, only a small number of inflammatory cells were detected in the superficial layers of the wound. In both groups, numerous capillaries were still present, and the collagen fiber bundles remained thin and arranged in parallel (Figures 5a, 5b). In the PBM and Gel+PBM groups, the granulation tissue exhibited more advanced signs of maturation, including a reduction in the number of fibroblasts and blood vessels, together with thickening of the collagen fiber bundles. In addition, the PBM group showed evidence of mild edema and the presence of isolated dilated blood vessels (Figures 5c, 5d).

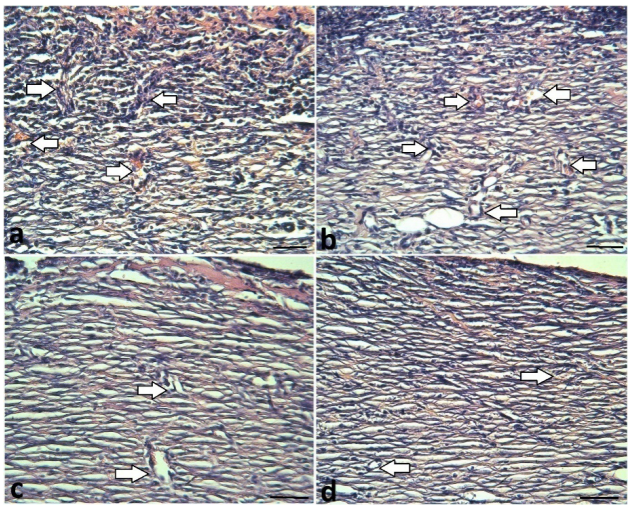

Figure 5. Wound areas in rats on day 14 of the experiment; groups: a) Con, b) Gel, c) PBM, d) Gel+PBM. Vessels in maturing granulation tissue (arrow). Hematoxylin and eosin. Scale bar 50 μm.

DISCUSSION

The combined use of nanomaterial-based hydrogels and PBM therapy may represent a promising strategy for optimizing the repair process through the modulation of various biomolecules. Among these, vascular cell adhesion molecule-1 (VCAM-1) plays an important role in wound healing. VCAM-1 is a glycoprotein expressed on endothelial and other cell types that mediates leukocyte adhesion and migration into the wound area, thereby facilitating tissue clearance and initiating the regenerative process. In response to inflammatory stimuli, pro-inflammatory cytokines, including TNF-α and IL-1β, induce the expression of VCAM-1 on endothelial cells. Activated VCAM-1 interacts with integrins expressed on leukocytes, promoting their transmigration from the bloodstream into the wound tissue [18].

The role of VCAM-1 in various pathological conditions has been extensively described in the literature. Increased expression of this glycoprotein has been reported in cardiovascular diseases, liver disorders, rheumatoid arthritis, and cancer [18]. In the present study, serum VCAM-1 levels were elevated in the Con group at all experimental time points following wound induction compared with those in intact animals. This increase reflects endothelial activation and the intensity of the inflammatory response associated with wound healing and is consistent with previous reports.

Limited data are available regarding the effects of PBM on VCAM-1 expression. Studies involving far-infrared radiation (FIR) have demonstrated that this modality reduces TNF-α-induced VCAM-1 expression in endothelial cells through activation of heme oxygenase-1 (HO-1) [19]. Similarly, phototherapy has been shown to reduce the levels of adhesion molecules, including VCAM-1, in patients with psoriasis, resulting in significant clinical improvement [20].

In the present study, PBM therapy was associated with lower serum VCAM-1 levels in the PBM group compared with those in the Con group. One possible mechanism may involve suppression of NF-κB-mediated VCAM-1 expression and normalization of intracellular reactive oxygen species (ROS) levels through mitochondrial activation. These effects may contribute to reduced endothelial inflammatory activity and diminished leukocyte adhesion.

The Gel group exhibited lower VCAM-1 levels than the Con group throughout the experimental period. Under certain conditions, the hydrogel containing $LaVO_4^{3+}$ nanoparticles and Ag NPs may contribute to reducing oxidative stress and the production of pro-inflammatory cytokines through the antioxidant properties of $LaVO_4^{3+}$ [10] and the anti-inflammatory effects of Ag NPs [21], thereby suppressing NF-κB activation in endothelial cells. This mechanism may result in reduced expression of membrane-bound VCAM-1 and its soluble form in serum, limiting excessive inflammation and promoting wound healing.

The most pronounced reduction in VCAM-1 levels was observed in the Gel+PBM group throughout the experimental period. PBM therapy has been shown to reduce ROS levels, inhibit NF-κB activation, decrease the production of pro-inflammatory cytokines, and enhance the expression of anti-inflammatory cytokines. The hydrogel may complement these effects. Together, these mechanisms may contribute to a marked reduction in VCAM-1 expression, thereby limiting excessive inflammation and promoting tissue regeneration. Histological findings further support improved wound healing in animals treated with the combined Gel+PBM regimen at all stages of the repair process.

Endothelin-1 (ET-1) is a potent vasoconstrictor peptide and is considered a marker of endothelial dysfunction. It is produced and secreted primarily by vascular endothelial cells. In addition to regulating vascular tone, ET-1 is involved in cell growth, inflammation, and other physiological processes [22]. ET-1 stimulates fibroblasts to synthesize extracellular matrix components, promotes interactions between monocytes and endothelial cells, and enhances endothelial inflammation by inducing the release of pro-inflammatory mediators, including TNF-α and IL-6 [23]. Therefore, ET-1 is regarded as a potential mediator of the systemic response to injury, and its serum concentration reflects changes occurring at the macrovascular level. Elevated ET-1 levels have been reported after myocardial infarction [24], in pulmonary hypertension [25], during various infectious processes [26], and in sepsis [27].

Our study demonstrated elevated serum ET-1 levels in the Con group throughout the experimental period compared with those in intact animals. During wound healing, ET-1 levels increase as a result of endothelial and immune cell activation induced by pro-inflammatory cytokines. ET-1 regulates vascular tone and promotes angiogenesis and fibroblast proliferation, thereby contributing to granulation tissue formation and scar development [22].

Limited data are available regarding the effects of PBM on ET-1 levels. For example, the combination of non-surgical periodontal therapy and PBM has been shown to significantly reduce salivary ET-1 levels in patients with periodontitis [28]. In the present study, lower serum ET-1 concentrations were observed in the PBM group compared with those in the Con group. PBM-induced activation of mitochondrial cytochrome c oxidase leads to increased ATP and nitric oxide (NO) production. Nitric oxide acts as a functional antagonist of ET-1 and may suppress its synthesis

in endothelial cells [29]. In addition, PBM reduces oxidative stress and decreases the secretion of pro-inflammatory cytokines, including TNF-α, IL-1β, and TGF-β1, which are important inducers of endothelin-1 production by endothelial cells. Consequently, reduced ET-1 levels may contribute to vasodilation, improved microcirculation, and enhanced tissue repair.

The Gel group also exhibited lower serum ET-1 levels than the Con group. This effect may be attributed to the combined influence of the nanoparticles on inflammation, oxidative stress, and endothelial activation. Similarly, animals receiving the combined Gel+PBM treatment demonstrated reduced ET-1 concentrations throughout the experimental period compared with the Con group. The decrease in ET-1 levels in this group may be associated with the complementary effects of PBM and the antioxidant properties of the nanoparticles. Together, these factors may reduce oxidative stress, which is a major inducer of ET-1 expression, suppress the production of pro-inflammatory cytokines involved in ET-1 synthesis, and promote restoration of vascular function through attenuation of oxidative stress and inflammation.

According to the histological findings, the PBM and Gel+PBM groups exhibited a more uniform distribution of newly formed blood vessels on day 3 compared with the other groups, indicating active formation of immature granulation tissue. By day 14, a reduction in the number of blood vessels was observed in the PBM and Gel+PBM groups, confirming the presence of maturing granulation tissue within the wound. These findings suggest activation of reparative processes, normalization of angiogenesis, and the absence of morphological features indicative of delayed or pathological wound healing.

Keratinocyte autocrine factor (KAF) investigated in the present study is identical to amphiregulin (AREG), as confirmed by N-terminal amino acid sequence analysis, antigenic cross-reactivity, and activity-blocking studies [30]. AREG is a ligand of the epidermal growth factor receptor (EGFR) and is considered a key mediator linking tissue injury, inflammation, and tissue regeneration, thereby contributing to both physiological wound healing and pathological fibrosis [31]. AREG is produced by keratinocytes, fibroblasts, and various immune cells [32,33]. These cells become activated during inflammation and tissue injury and release AREG, which promotes tissue regeneration through EGFR-mediated signaling pathways.

Macrophage-derived AREG regulates the differentiation of pericytes into collagen-producing myofibroblasts by inducing TGF-β activation, which represents a key step in extracellular matrix formation and wound repair [34]. Therefore, AREG plays an important role in tissue regeneration, modulation of inflammation, and immune responses.

Available evidence indicates that AREG is actively involved in tissue injury and repair processes, predominantly at the local level. In the present study, we aimed to investigate the systemic circulation of AREG during wound healing.

In the present study, serum KAF/AREG levels were elevated in the Con group on day 3 after surgery compared with those in intact animals. However, no significant differences in KAF/AREG concentrations were observed between wounded and intact animals on days 7 and 14. Amphiregulin (AREG) is expressed by keratinocytes, macrophages, immune cells, and fibroblasts in response to tissue injury. Upon release, AREG binds to epidermal growth factor receptor (EGFR) and activates TGF-β, thereby stimulating cell proliferation and migration, angiogenesis, and myofibroblast differentiation, which collectively contribute to tissue repair and wound healing. Nevertheless, the biological activity of AREG is predominantly localized to the site of injury, and only a small proportion enters the systemic circulation, reflecting the extent of tissue damage and local reparative activity.

To the best of our knowledge, no studies have directly investigated the effects of PBM therapy on serum KAF/AREG levels. In the present study, serum KAF/AREG concentrations were slightly higher in animals treated with PBM than in the Con group; however, these differences did not reach statistical significance ($p > 0.05$). PBM influences mitochondrial activity, increases ATP production, and activates multiple transcription factors. These processes may stimulate the expression of growth factors, including AREG, thereby promoting tissue regeneration and wound healing. Likewise, no significant increase in KAF/AREG levels was observed in the Gel group ($p > 0.05$). The highest KAF/AREG concentrations were observed in the Gel+PBM group on days 3 and 7; however, these differences were also not statistically significant ($p > 0.05$). The nanoparticles incorporated into the hydrogel may create a microenvironment in which PBM could modulate AREG-related signaling pathways, although this hypothesis was not directly investigated in the present study.

Our findings suggest that, despite the important local role of AREG in tissue regeneration, serum AREG levels do not undergo marked changes during the wound healing process.

Although the combined treatment produced more pronounced effects than either therapy alone, further studies using appropriate statistical interaction models are required to determine whether these effects are truly synergistic.

CONCLUSIONS

1. Serum levels of ET-1 and VCAM-1 increased during the early stages of wound healing, consistent with endothelial activation and inflammatory cell recruitment at the site of injury. PBM therapy, hydrogel treatment, and their combination were associated with modulation of ET-1 and VCAM-1 levels, which may contribute to the establishment of a more favorable microenvironment for wound healing. Although KAF/AREG may participate in keratinocyte-related signaling during re-epithelialization, this mechanism was not directly confirmed in the present study and warrants further investigation.
2. Histological findings indicated that the combined application of $Ag/LaVO_4^{3+}$ NPs hydrogel and PBM therapy was associated with more organized granulation tissue formation, earlier vascularization, and subsequent tissue maturation. The observed attenuation of the inflammatory response during the early stage of repair may facilitate a more timely transition to the proliferative and remodeling phases of wound healing.

3. Overall, these findings suggest that the combined therapeutic approach may have potential for improving wound healing. However, further studies are required to elucidate the underlying mechanisms and evaluate its translational potential.

CONFLICT OF INTEREST

The authors declare that they have no conflicts of interest.

FUNDING

This work was supported by the Ministry of Health of Ukraine through state budget funding. The study constitutes a part of the research project conducted at Kharkiv National Medical University entitled "Activation of reparative processes in chronic wounds using biomaterials immobilized on hydrogels and photobiomodulation therapy" (state registration No. 0124U000579, 2024-2026).

ETHICAL APPROVAL

The study protocol was approved by the Bioethics Committee of Kharkiv National Medical University, Ukraine (Protocol No. 17, March 6, 2024).

ORCID iDs

Sergey Pavlov https://orcid.org/0000-0002-3952-1511
Marina Kumetchko https://orcid.org/0000-0002-9153-2461
Olga Litvinova https://orcid.org/0000-0002-4558-6979
Nataliia Babenko https://orcid.org/0000-0003-3117-8146
Vladimir Klochkov https://orcid.org/0000-0002-8080-1195
Svitlana Yefimova https://orcid.org/0000-0003-2092-1950
Igor Kolisnyk https://orcid.org/0000-0002-9442-858X

REFERENCES

1. Secco J, Spinazzola E, Pittarello M, Ricci E, Pareschi F. Clinically validated classification of chronic wounds method with memristor-based cellular neural network. *Sci Rep.* 2024;14(1):30839. doi: 10.1038/s41598-024-81521-9.
2. Falanga V, Isseroff RR, Soulika AM, Romanelli M, Margolis D, Kapp S, et al. Chronic wounds. *Nat Rev Dis Primers*. 2022;8(1):50. doi: 10.1038/s41572-022-00377-3.
3. Litvinova O, Kumetchko M, Pavlov S, Babenko N, Kolisnyk I. Problems of healing soft tissue injuries. *East Ukr Med J.* 2025;13(1): 1-13. doi: 10.21272/eumj.2025;13(1):1-13.
4. Sen CK. Human wound and its burden: updated 2025 compendium of estimates. *Adv Wound Care* (New Rochelle). 2025;14(9):429-438. doi: 10.1177/21621918251359554.
5. Shevchenko R, Pavlov S, Babenko N, Kumetchko M, Litvinova O, Torianyk I. Effect of photobiomodulation therapy on regulating reparative processes of chronic wounds at the inflammation stage. *Biomédica*. 2026;46(3). doi: 10.7705/biomedica.7820.
6. Colombo E, Signore A, Aicardi S, Zekiy AO, Utyuzh AS, Benedicenti S, et al. Experimental and clinical applications of red and near-infrared photobiomodulation on endothelial dysfunction: a review. *Biomedicines*. 2021;9(3):274. doi: 10.3390/biomedicines9030274.
7. Sheikh-Oleslami S, Tao B, D'Souza J, Butt F, Suntharalingam H, Rempel L, et al. A review of metal nanoparticles embedded in hydrogel scaffolds for wound healing *in vivo*. *Gels*. 2023;9(7):591. doi: 10.3390/gels9070591.
8. Singh M, Thakur V, Kumar V, Raj M, Gupta S, Devi N, et al. Silver nanoparticles and its mechanistic insight for chronic wound healing: review on recent progress. *Molecules*. 2022;27(17):5587. doi: 10.3390/molecules27175587.
9. Gunasekaran T, Nigusse T, Dhanaraju MD. Silver nanoparticles as real topical bullets for wound healing. *J Am Coll Clin Wound Spec.* 2012;3(4):82-96. doi: 10.1016/j.jcws.2012.05.001.
10. Yefimova SL, Maksimchuk PO, Seminko VV, Kavok NS, Klochkov VK, Hubenko KA, et al. Janus-faced redox activity of LnVO4+ (Ln = Gd, Y, and La) nanoparticles. *J Phys Chem C*. 2019;123(24). doi: 10.1021/acs.jpcc.9b03040.
11. Klochkov VK, Sedyh OO, Grygorova GV, Karpenko NO, Maksimchuk PO, Pavlov SB, et al. Plasmon-enhanced photocatalysis and antimicrobial activity of Ag/LaVO4+ nanoparticle gel for wound healing. *Funct Mater.* 2025;32(4):663-671. doi: 10.15407/fm32.04.663.
12. Kot Y, Klochkov V, Prokopiuk V, Sedyh O, Tryfonyuk L, Grygorova G, et al. GdVO4+ and LaVO4+ nanoparticles exacerbate oxidative stress in L929 cells: potential implications for cancer therapy. *Int J Mol Sci.* 2024;25(21):11687. doi: 10.3390/ijms252111687.
13. Gonca S, Yefimova S, Dizge N, Tkachenko A, Özdemir S, Prokopiuk V, et al. Antimicrobial effects of nanostructured rare-earth-based orthovanadates. *Curr Microbiol*. 2022;79(9):254. doi: 10.1007/s00284-022-02947-w.
14. Klochkov VK, Malyshenko AI, Sedykh OO, Malyukin YV. Wet chemical synthesis and characterization of luminescent colloidal nanoparticles: ReVO4+ (Re = La, Gd, Y) with rod-like and spindle-like shape. *Funct Mater.* 2011;18(1):111-115.
15. Grygorova G, Klochkov V, Sedyh O, Malyukin Y. Aggregative stability of colloidal ReVO4+ (Re = La, Gd, Y) nanoparticles with different particle sizes. *Colloids Surf A Physicochem Eng Asp*. 2014;457:495-501. doi: 10.1016/j.colsurfa.2014.06.024.
16. Loiseau A, Asila V, Boitel-Aullen G, Lam M, Salmain M, Boujday S. Silver-based plasmonic nanoparticles and their use in biosensing. *Biosensors* (Basel). 2019;9(2):78. doi: 10.3390/bios9020078.
17. Fan W, Bu Y, Song X, Sun S, Zhao X. Selective synthesis and luminescent properties of monazite- and zircon-type LaVO4 (Ln = Eu, Sm, and Dy) nanocrystals. *Cryst Growth Des.* 2007;7(11):2361-2366. doi: 10.1021/cg060807o.
18. Singh V, Kaur R, Kumari P, Pasricha C, Singh R. ICAM-1 and VCAM-1: gatekeepers in various inflammatory and cardiovascular disorders. *Clin Chim Acta*. 2023;548:117487. doi: 10.1016/j.cca.2023.117487.
19. Lin CC, Liu XM, Peyton K, Wang H, Yang WC, Lin SJ, et al. Far infrared therapy inhibits vascular endothelial inflammation via the induction of heme oxygenase-1. *Arterioscler Thromb Vasc Biol.* 2008;28(4):739-745. doi: 10.1161/ATVBAHA.107.160085.
20. Cabrijan L, Lipozenčić J, Batinac T, Lenković M, Stanić-Zgombić Z. Influence of PUVA and UVB radiation on expression of ICAM-1 and VCAM-1 molecules in psoriasis vulgaris. *Coll Antropol.* 2008;32 Suppl 2:53-56.
21. Luceri A, Francese R, Lembo D, Ferraris M, Balagna C. Silver nanoparticles: review of antiviral properties, mechanism of action and applications. *Microorganisms*. 2023;11(3):629. doi: 10.3390/microorganisms11030629.
22. Makino K, Jinnin M, Aoi J, Kajihara I, Makino T, Fukushima S, et al. Knockout of endothelial cell-derived endothelin-1 attenuates skin fibrosis but accelerates cutaneous wound healing. *PLoS One*. 2014;9(5). doi: 10.1371/journal.pone.0097972.
23. Walczak M, Fedorowicz A, Chłopicki S, Szymura-Oleksiak J. Determination of endothelin-1 in rats using a high-performance liquid chromatography coupled to electrospray tandem mass spectrometry. *Talanta*. 2010;82(2):710-718. doi: 10.1016/j.talanta.2010.05.037.
24. Hartopo AB, Sukmasari I, Puspitawati I, Setianto BY. Serum endothelin-1 correlates with myocardial injury and independently predicts adverse cardiac events in non-ST-elevation acute myocardial infarction. *Int J Vasc Med*. 2020;2020:9260812. doi: 10.1155/2020/9260812.
25. Shao D, Park JE, Wort SJ. The role of endothelin-1 in the pathogenesis of pulmonary arterial hypertension. *Pharmacol Res.* 2011;63(6):504-511. doi: 10.1016/j.phrs.2011.03.003.
26. Freeman BD, Machado FS, Tanowitz HB, Desruisseaux MS. Endothelin-1 and its role in the pathogenesis of infectious diseases. *Life Sci*. 2014;118(2):110-119. doi: 10.1016/j.lfs.2014.04.021.
27. Piechota M, Banach M, Irzmanski R, Barylski M, Piechota-Urbanska M, Kowalski J, et al. Plasma endothelin-1 levels in septic patients. *J Intensive Care Med*. 2007;22(4):232-239. doi: 10.1177/0885066607301444.

28. Kulkarni S, Zope S, Suragimath G, Varma S, Kale A. Comparative assessment of salivary endothelin-1 levels in periodontitis subjects following non-surgical periodontal therapy (NSPT) with adjunctive photobiomodulation and NSPT alone: a prospective interventional study. *Bull Stomatol Maxillofac Surg.* 2025;21(3):222-232. doi: 10.58240/1829006X-2025.3-223.
29. Iglarz M, Clozel M. Mechanisms of ET-1-induced endothelial dysfunction. *J Cardiovasc Pharmacol.* 2007;50(6):621-628. doi: 10.1097/FJC.0b013e31813c6cc3.
30. Cook PW, Mattox PA, Keeble WW, Pittelkow MR, Plowman GD, Shoyab M, et al. A heparan sulfate-regulated human keratinocyte autocrine factor is similar or identical to amphiregulin. *Mol Cell Biol.* 1991;11(5):2547-2557. doi: 10.1128/MCB.11.5.2547-2557.1991.
31. Sisto M, Lisi S. Amphiregulin and fibrosis: existing evidence and future directions. *Int J Mol Sci.* 2025;26(16):7678. doi: 10.3390/ijms26167678.
32. Loffredo LF, Kustagi A, Ringham OR, Li F, de Los Santos-Alexis K, Saqi A, et al. Heparan sulfate regulates amphiregulin programming of tissue reparative lung mesenchymal cells during influenza A virus infection in mice. *Nat Commun.* 2025;16(1):2129. doi: 10.1038/s41467-025-57362-z.
33. Zaiss DMW, Gause WC, Osborne LC, Artis D. Emerging functions of amphiregulin in orchestrating immunity, inflammation, and tissue repair. *Immunity.* 2015;42(2):216-226. doi: 10.1016/j.immuni.2015.01.020.
34. Minutti CM, Modak RV, Macdonald F, Li F, Smyth DJ, Dorward DA, et al. A macrophage-pericyte axis directs tissue restoration via amphiregulin-induced transforming growth factor beta activation. *Immunity.* 2019;50(3):645-654.e6. doi: 10.1016/j.immuni.2019.01.008.